Examination of the product channels in the reactions of NH(a 1Δ) with H2 and D2

Atsumu Tezaki, Satoru Okada, and Hiroyuki Matsui

Citation: The Journal of Chemical Physics **98**, 3876 (1993); doi: 10.1063/1.464015
View online: http://dx.doi.org/10.1063/1.464015
View Table of Contents: http://scitation.aip.org/content/aip/journal/jcp/98/5?ver=pdfcov
Published by the AIP Publishing

Examination of the product channels in the reactions of NH($a\ ^1\Delta$) with H_2 and D_2

Atsumu Tezaki, Satoru Okada, and Hiroyuki Matsui
Department of Reaction Chemistry, The University of Tokyo, Hongo, Bunkyo-ku, Tokyo 113 Japan

(Received 24 September 1992; accepted 18 November 1992)

A flash photolysis study (193 nm) of HNCO has been conducted and the mechanisms of the reactions $NH(a\ ^1\Delta)+H_2\rightarrow NH_2+H$(1) and $NH(a\ ^1\Delta)+D_2\rightarrow$products (2) have been examined in detail at 295±3 K by monitoring $NH(a\ ^1\Delta)$, H, D, NH_2, and their D substituents via the laser induced fluorescence technique. From the pseudo-first-order analysis of the decay rate for $NH(a\ ^1\Delta)$, rate constants have been determined as $k_1=(3.96\pm0.17)\times10^{-12}$ and $k_2=(2.62\pm0.08)\times10^{-12}$. (All the rate constants are expressed in units of cm^3 $molecule^{-1}$ s^{-1}.) These rate constants are consistent with those determined from the time dependence of H and D atoms: they are $k_1=(3.76\pm0.70)\times10^{-12}$ and $k_2=(2.78\pm0.17)\times10^{-12}$. No pressure dependence has been observed for 10–100 Torr He. The branching fraction for H and D atoms as products for reaction (2) has been found to be [H]/[D] =0.24/0.76, where D production is more abundant than statistically predicted. This indicates that reaction (2) is dominated by insertion of $NH(a\ ^1\Delta)$ into the D_2 bond, but vibrational energy of the reaction intermediate NHD_2 is still localized in newly formed N–D bonds before it passes through the exit barrier into NHD+D or ND_2+H channels. $NH_2(\tilde{X}\ ^2B_1)$ was observed in (0,0,0) and (0,1,0) vibrational states as a product of reaction (1), and the observed time dependence of both vibrational states could be satisfactorily simulated by solving the master equation for vibrational relaxation of NH_2. This analysis has indicated that the vibrational energy partitioning in the product NH_2 is nearly statistical.

I. INTRODUCTION

Reactions of metastable singlet imidogen radical, $NH(a\ ^1\Delta)$, have interested many chemical kineticists because both electronic excitation and spin states exhibit crucial roles in chemical reactivity.[1–17] $NH(a\ ^1\Delta)$ can react through insertion into a chemical bond of a colliding molecule in many cases, but direct abstraction sometimes competes with this: also, electronic quenching to ground state $NH(X\ ^3\Sigma^-)$ is important for consuming $NH(a\ ^1\Delta)$. Reaction of $NH(a\ ^1\Delta)$ with H_2

$$NH(a\ ^1\Delta)+H_2\rightarrow NH_2+H \qquad (1)$$

is one of the simplest examples. The overall rate constant for this reaction has been measured by means of direct observation of the $NH(a\ ^1\Delta)$ decay rate[15–17] and reported to be in the range 2.9–4.6$\times10^{-12}$ cm^3 $molecule^{-1}$ s^{-1}. The rate constant for (1) is considerably slow compared to those for other isoelectronic systems, $O(^1D)+H_2$ and $CH_2(\tilde{a}\ ^1A_1)+H_2$ (overall rate constants are about 10^{-10} cm^3 $molecule^{-1}$ s^{-1} for both cases[18–21]).

The $O(^1D)+H_2$ reaction dynamics has been extensively studied whereby rotational and vibrational energy distributions in the product OH radical was measured.[22–26] Also, the branching fraction for H and D atoms has been found for $O(^1D)+HD\rightarrow OH(OD)+D(H)$.[24,27] Semiempirical[28] and *ab initio*[29–32] calculations for the potential energy surface have been performed for these reaction systems. By means of trajectory calculations on the model potential surfaces, the reaction mechanism, internal energy distribution in OH, and branching fraction for H and D atoms [in the case of $O(^1D)+HD$] have been examined.[28,30,33–35] Although it is now widely accepted that insertion of $O(^1D)$ into the H_2 bond dominates over the direct abstraction channel, a serious discrepancy in predictions using the model potential surfaces of the branching fraction in the $O(^1D)+HD$ reaction was indicated.[34,35]

There has been almost no experimental information, in contrast, on the details of the mechanism for reaction (1) (insertion or direct abstraction), but a substantial contribution of direct abstraction in the reaction $NH(a\ ^1\Delta)$ + paraffins has been indicated,[6,7] as is also analogous to the reactions $O(^1D)$ + paraffins.[36]

Therefore, in addition to determining the overall rate constant from the disappearance of $NH(a\ ^1\Delta)$ in reaction (1), it may be meaningful to measure the rates and relative concentrations of H and D atoms and also those of NHD and ND_2 produced in

$$NH(a\ ^1\Delta)+D_2\rightarrow NHD+D, \qquad (2a)$$

$$\rightarrow ND_2+H, \qquad (2b)$$

so as to clarify the mechanism of these important reactions.

II. EXPERIMENTAL SECTION

The experimental setup was essentially the same as that of our previous work:[14,37] in brief, all the kinetic information in this study was obtained by means of a laser flash photolysis/LIF scheme in a quasistatic reaction cell at room temperature (295±3 K). The observed species are summarized in Table I. H and D atoms were detected by a vacuum uv LIF technique. Tunable vuv light pulse in the Lyman-α region was generated by a frequency tripling

 0021-9606/93/053876-08$06.00

TABLE I. Observed species.[a]

Species	Transition		Wavelength (nm)
NH ($a\,^1\Delta$)		$c\,^1\Pi$–$a\,^1\Delta$ (0′–0″)	325
NH ($X\,^3\Sigma^-$)		$A\,^3\Pi$–$X\,^3\Sigma^-$ (0′–0″)	336
H		Lyman α	121.57
D		Lyman α	121.53
NH_2	$\tilde{A}\,^2A_1$–$\tilde{X}\,^2B_1$	(0,9,0)′–(0,0,0)″Σ	598
		(0,9,0)′–(0,0,0)″Δ	602
		(0,12,0)′–(0,0,0)″Π	516
		(0,14,0)′–(0,1,0)″Π	507
ND_2	$\tilde{A}\,^2A_1$–$\tilde{X}\,^2B_1$	(0,12,0)′–(0,0,0)″Π	603
NHD	$\tilde{A}\,^2A_1$–$\tilde{X}\,^2B_1$	(0,10,0)′–(0,0,0)″Π	604

[a]Upper state v_2 of NH_2, ND_2, and NHD are denoted by linear notation, where $v_2(\text{linear})=2v_2(\text{bent})+K_a+1$.

method: a uv laser beam at around 364.8 nm generated by a dye laser (Lambda Physik LPD3002E/LPX110i) was focused in a Kr cell at a pressure of 60 Torr, and the vuv generation was probed by monitoring ionization signals using a cell filled with 2% NO in He of 40 Torr, set behind the reaction cell. By scanning the wavelength, absorption for Lyman-α lines was measured to estimate the absolute concentrations for H and D atoms with known absorption cross section. By means of a standard tunable pulsed laser system (Spectra-Physics PDL-3/Quanta-Ray DCR-2), LIF excitation spectra and their time dependence were measured for NH($a\,^1\Delta$) or NH_2, NHD, and $ND_2(\tilde{X}\,^2B_1)$ in the reactions (1) and (2).

NH($a\,^1\Delta$) radicals were generated by photolysis of isocyanic acid (HNCO) with an ArF laser (Questek 2220) irradiation at 193 nm with a typical fluence of 10 mJ/cm^2 into a Pyrex cell of about 2 cm i.d. The partial pressure of HNCO was in the range of 0.5–5 mTorr, and the total pressure of the He buffered mixture was maintained at 10 Torr with 200 sccm flow rate, except for the measurements on the total pressure dependence of the reaction rate.

HNCO was synthesized and purified as previously.[14] Research grade H_2, D_2 (99%) (Nihon-Sanso) were used without further purification. Blank tests revealed that no LIF signals for NH($a\,^1\Delta$) and OH, due to impurities, could be detected.

III. EXPERIMENTAL RESULTS

A. Overall rate constants for reactions (1) and (2)

Typical time profiles of NH($a\,^1\Delta$) and H atom in a photolysis of the $HNCO/H_2$ mixture are shown in Figs. 1(a) and 1(b), respectively. The decay of NH($a\,^1\Delta$) LIF intensity showed a single exponential profile. On the other hand, the LIF intensity of H atoms showed a fast rise at the moment of photolysis ($t=0$), then gradually increased toward pseudosteady level with almost the same rate for NH($a\,^1\Delta$) consumption. This was a result of the following processes:

$$\text{HNCO}+h\nu\rightarrow\text{NH}(a\,^1\Delta)+\text{CO}, \quad \text{(i-a)}$$

$$\rightarrow\text{H}+\text{NCO}, \quad \text{(i-b)}$$

$$\text{NH}(a\,^1\Delta)+\text{H}_2\rightarrow\text{NH}_2+\text{H}. \quad (1)$$

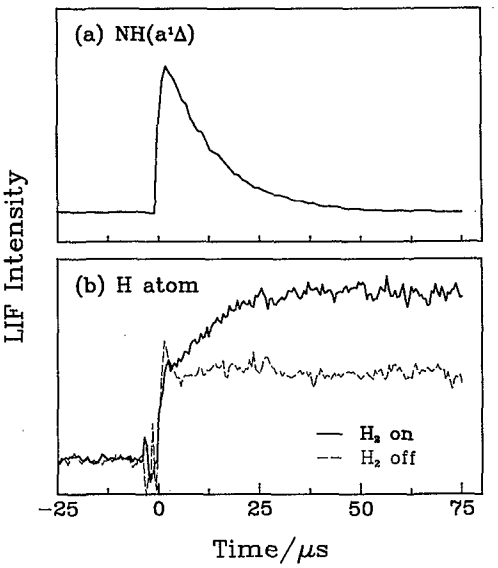

FIG. 1. Transient LIF signals of NH($a\,^1\Delta$) and H in ArF laser photolysis of $HNCO/H_2$ mixture. (a) NH($a\,^1\Delta$); (b) H atom. Sample gas: 5 mTorr HNCO with/without 0.61 Torr H_2 in He (10 Torr total pressure).

As the consumption rate of H atoms through the consecutive reactions of heterogeneous loss processes at the wall was found to be sufficiently slower (about 1500 s^{-1}), it is reasonable to assume that the yield of H atoms is 100% in reaction (1) at the observed steady level. Then from the ratio of the initial to final concentrations for H atoms, branching ratio for the 193 nm photolysis of HNCO, reactions (i-a), and (i-b), was determined to be $(0.64\pm0.01)/(0.36\pm0.01)$. This result was an average value for six independent measurements. No clear dependence on the photolysis energy was observed between 5 and 20 mJ/cm^2 of the ArF laser fluence. This branching is not consistent with that of previous work,[38] in which the branching fraction for reaction (i-b) was suggested to be less than 10% via LIF measurement of NCO. The photolysis branching fraction determined in this study is somewhat similar to that of HN_3 photolysis at 193 and 248 nm, in which the yield of H atoms was reported to be larger than that suggested previously.[39]

The dependence of the decay rate for NH($a\,^1\Delta$) on the concentration of added D_2 in $HNCO/D_2/He$ mixtures was also measured. In these mixtures, H and D atoms were separately monitored as products of reactions (2a) and (2b). Typical examples of the profiles are shown in Fig. 2. As shown in the upper panel, if D_2 was not present in the sample gas, the concentration of H atoms remained constant at the same level of that initially formed by the photolysis, but addition of D_2 clearly resulted in a gradual increase to another steady level, suggesting a contribution of reaction (2b).

On the other hand, D atoms were not formed at the moment of photolysis both with and without addition of D_2 to the samples, as shown in the lower panel of Fig. 2. Zero level was kept thereafter when D_2 was absent; in contrast, the concentration of D gradually increased to a

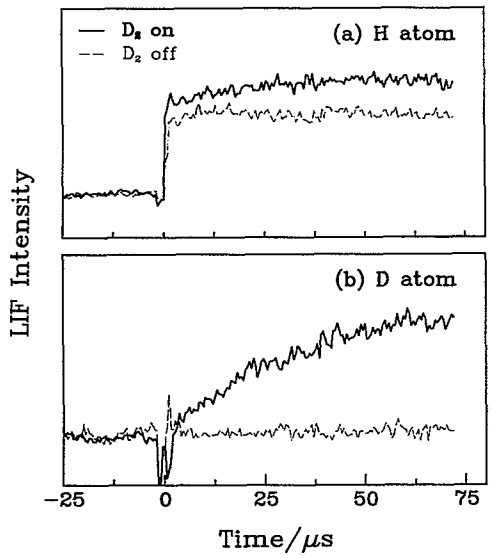

FIG. 2. Vacuum ultraviolet-LIF signals of product H atom and D atom in the photolysis of HNCO/D_2 mixture. Sample gas: 5 mTorr HNCO with/without 0.27 Torr D_2 in He (10 Torr total pressure).

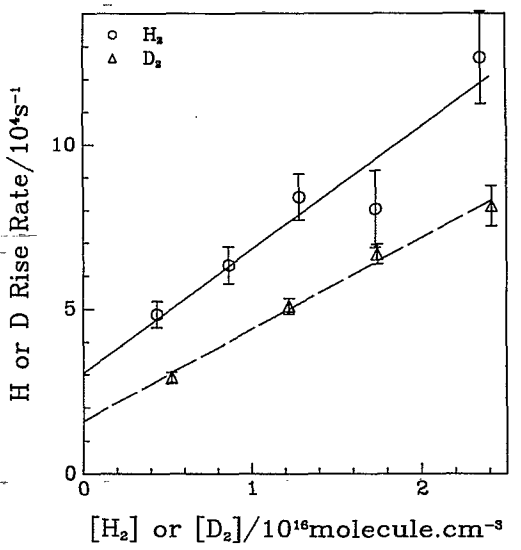

FIG. 4. Pseudo-first-order analysis of the rate constants using the rise rate of H atom (for k_1) and D atom (for k_2). [HNCO] is 5 mTorr in 10 Torr He.

steady level when D_2 was present. Weak traces of ND($a\,^1\Delta$) were detected but their intensity was estimated to be below 1% of that of NH($a\,^1\Delta$) at the same experimental conditions. These observations indicate that H/D exchange by a catalytic reaction in the HNCO/D_2 mixture to form DNCO prior to the photolysis was negligible.

The decay rates of NH($a\,^1\Delta$) correlated linearly with the concentration of H_2 or D_2, as shown in Fig. 3: from the slopes of the pseudo-first-order decay rate of NH($a\,^1\Delta$), the overall rate constants for reactions (1) and (2) were determined to be $k_1=(3.96\pm0.17)\times10^{-12}$ and $k_2=(2.62\pm0.08)\times10^{-12}$ cm^3 molecule^{-1} s^{-1} (errors indicate 2σ deviation). It is noted that the physical quenching process

$$\mathrm{NH}(a\,^1\Delta)+\mathrm{H_2}\rightarrow\mathrm{NH}(X\,^3\Sigma^-)+\mathrm{H_2} \qquad (3)$$

did not contribute to the observed disappearance rate for NH($a\,^1\Delta$), since the rate constant of reaction (3) is reported to be sufficiently slow at the present experimental conditions;[15–17] also, no LIF signal due to NH($X\,^3\Sigma^-$) could be detected for the typical experimental conditions in this study, where the relative intensities for NH($X\,^3\Sigma^-$) and NH($a\,^1\Delta$) had been calibrated by using Xe as an effective quencher in the photolysis of HNCO.[14]

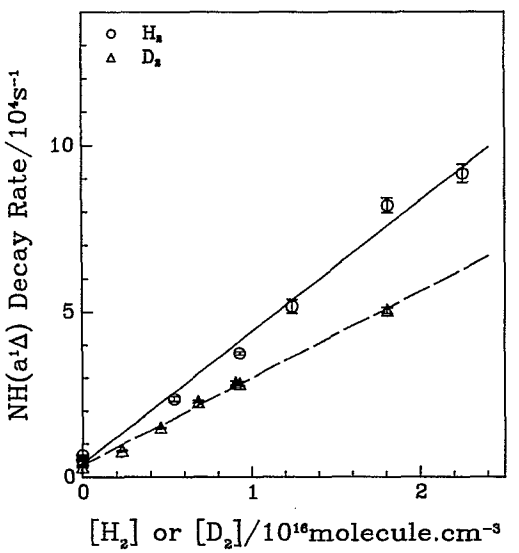

FIG. 3. Pseudo-first-order analysis of the rate constants of NH($a\,^1\Delta$) + H_2 [reaction (1)], and NH($a\,^1\Delta$) + D_2 [reaction (2)] using the decay rate of NH($a\,^1\Delta$). [HNCO] is 1 mTorr in 10 Torr He.

Also, the rates of formation of H and D atoms in these reactions are plotted against the concentrations of H_2 and D_2 in Fig. 4. The slopes of these plots again give the overall rate constants for these reactions; they are expressed as $k_1=(3.76\pm0.70)\times10^{-12}$ and $k_2=(2.78\pm0.17)\times10^{-12}$ cm^3 molecule^{-1} s^{-1} from the rates of formation of H and D atoms, respectively. As was noted above, an interference by the initial formation of H atoms by the photolysis of HNCO resulted in a larger error in the estimated rate constant for reaction (1) than that for reaction (2). However, the rate constants estimated by means of two ways in this study agree very well each other. They are also consistent with previous measurements[15–17] for reaction (1), as summarized in Table II. No previous measurement on reaction (2) has been found in our literature search.

The observed isotope effect, $k_2/k_1=0.66\pm0.02$ determined from the decay of NH($a\,^1\Delta$), or 0.74 ± 0.12 determined from the formation of H and D atoms, is very close to the inverse of the square root of the reduced mass of the collision pairs; i.e., $[\mu(\mathrm{NH\text{–}H_2})/\mu(\mathrm{NH\text{–}D_2})]^{-1/2}=0.75$; this seems to be consistent with the insertion mechanism, i.e., if the reaction proceeds by the association of NH and $H_2(D_2)$ with a low barrier in the entrance channel of the

TABLE II. Summary of rate constants.

Initiation	Detection	T (K)	Rate const.[a]	Ref.
$k_1=k\{NH(a\,^1\Delta)+H_2\}$				
266 nm LFP HN_3	NH(c–a) LIF	300±5	4.6±0.4	15
193 nm LFP HNCO	NH(c–a) LIF		2.9±0.6	16
193 nm LFP HN_3	NH(a–X) PP	296±3	3.4±0.2	17
193 nm LFP HNCO	NH(c–a) LIF	295±5	4.0±0.2	This work
193 nm LFP HNCO	H(Ly α) LIF	295±5	3.8±0.7	This work
$k_2=k\{NH(a\,^1\Delta)+D_2\}$				
193 nm LFP HNCO	NH(c–a) LIF	295±5	2.6±0.1	This work
193 nm LFP HNCO	D(Ly α) LIF	295±5	2.8±0.2	This work

[a]Units in 10^{-12} cm^3 molecule^{-1} s^{-1}; LFP: laser flash photolysis, PP: phosphorescence.

reaction coordinate, then the rate constant should be approximately proportional to the collision frequency.

B. Branching fraction of H and D in the reaction $NH(a\,^1\Delta)+D_2$

In order to determine a branching fraction of D and H atoms produced in the reactions (2a) and (2b), respectively, LIF line shapes of H and D were repeatedly traced for the mixtures of HNCO with various partial pressure of D_2 at a fixed reaction time of 75 μs after the photolysis.

The concentrations for H and D atoms were directly compared from the integrated line strengths without correction, even though the difference in the Doppler widths gives a change in the peak height as a function of spectral width of the probe laser. The relative intensities for H and D atoms were normalized by $[H]_0$ (the initial concentration of H atoms produced in the photolysis of HNCO) as shown in Fig. 5; the net amount of H atoms produced in reaction (2b) was evaluated by comparing the LIF intensities of H atoms with and without addition of D_2 as illustrated in the upper panel in Fig. 2. The same procedures were repeatedly taken at both 10 and 30 Torr of total pressure, and in the range of $1–3\times10^{16}$ molecule/cm^3 of D_2 partial pressure. The average branching fraction is summarized as

$$k_{2a}/k_{2b}=[D]/[H]=3.12\pm0.60$$

or

$$k_{2a}/(k_{2a}+k_{2b})=0.76\pm0.04.$$

Furthermore, no dependence of the branching fraction on the total pressure up to 100 Torr was found.

The solid and dashed curves shown in Fig. 5 represent the calculated concentrations of H and D atoms at $t=75$ μs, respectively, where the above branching fraction together with the rate constant of $k_2=2.62\times10^{-12}$ cm^3 molecule^{-1} s^{-1} [determined from the decay rate of $NH(a\,^1\Delta)$] were employed. The simulation agrees very well with the observed dependence of [H] and [D] on $[D_2]$.

This is the first direct evidence that the insertion reaction is the main channel for $NH(a\,^1\Delta)+D_2$ since H atoms should not be emitted if only direct abstraction takes place. The fact that neither the [H]/[D] ratio nor the net amount of H and D atoms produced in reaction (2) depend on the total pressure, implies that the lifetime of excited NHD_2 is sufficiently short and it cannot be collisionally stabilized before it decomposes into NHD+D or ND_2+H in this pressure range. The deviation of the observed branching fraction from a statistical prediction is discussed later.

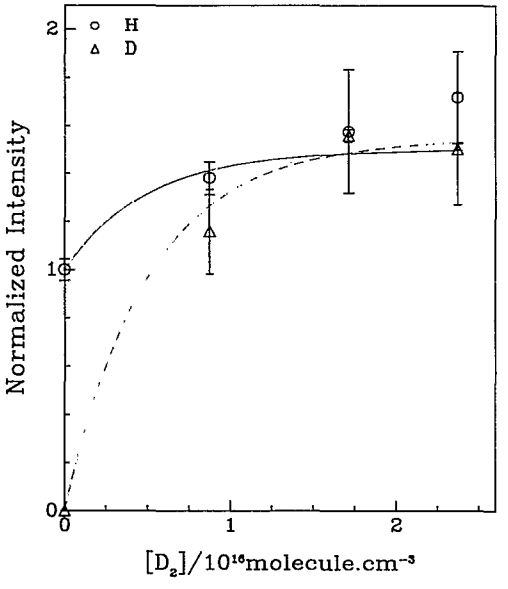

FIG. 5. The yields of H and D atoms as the products in reaction (2). Delay time was fixed at 75 μs after photolysis. The solid and dashed curves are analytical solutions using the rate constant k_2 obtained in this work where the D/H branching ratio was fitted as 3.05:1.

C. Rate of formation of NH_2

Laser excitation spectra of NH_2, NHD, and ND_2 produced in reactions (1) and (2) were observed in the wavelength range of 598–605 nm, where the spectral lines for all these species lie close together.[40–42] Examples of the spectra are shown in Fig. 6: only NH_2 was detected in HNCO/H_2 mixtures as shown in the upper panel, and in the lower panel, both NHD and ND_2 were assigned in HNCO/D_2 mixtures. It seems that NHD is more populous than ND_2 from the intensities of these excitation spectra, which is consistent with the observation of H and D atoms as stated above.

Time profiles of NH_2 formed in the $NH(a\,^1\Delta)+H_2$ reaction are shown in Fig. 7, where the 2_{12}–2_{02} rotational line of the $(\tilde{A}$–$\tilde{X})$ (0,12,0)–(0,0,0)Π band at 516.27 nm and the 2_{12}–2_{02} line of the $(\tilde{A}$–$\tilde{X})$ (0,14,0)–(0,1,0)Π band at 507.76 nm (Ref. 43) were monitored. In this figure, curves (a) and (b) are the profiles of (0,0,0) and (0,1,0), respectively. It should be noted that this experimental condition is the same as that shown in Fig. 1: formation of NH_2 $(\tilde{X})$(0,0,0) is much slower than consumption of $NH(a\,^1\Delta)$. Obviously, the delay was caused by the vibrational relaxation of the excited NH_2 to the ground state.

Trace (c) in the same figure was obtained when 1 Torr CF_4 was added to the same gas mixture: the transient LIF intensity for NH_2(0,0,0) revealed a single exponential profile, and the formation rate agrees with the decay rate of

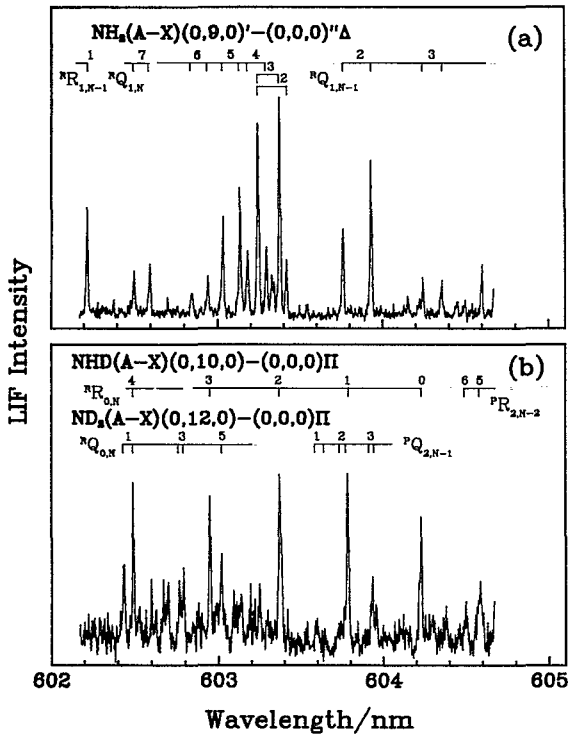

FIG. 6. Laser induced excitation spectra of products in the photolysis of (a) 10 mTorr HNCO/0.67 Torr H_2, and (b) 10 mTorr HNCO/0.67 Torr D_2. Rotational lines of NH_2 in (a), and both NHD and ND_2 are shown in (b) (See Refs. 40–42). Linear notations are used for upper state bending vibrations.

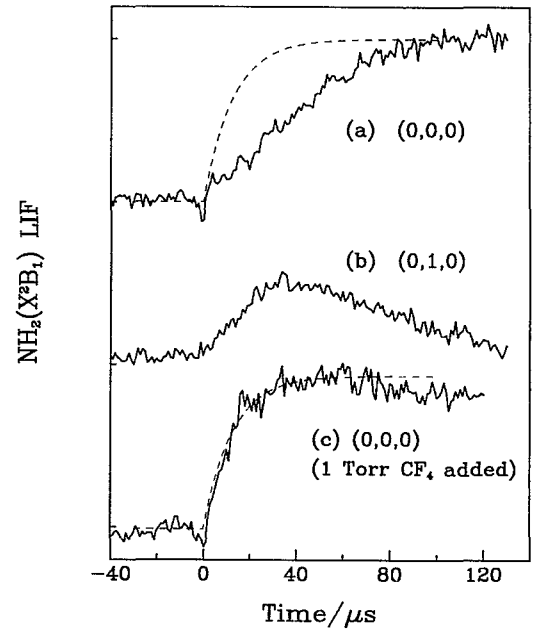

FIG. 7. The transient LIF intensity of $NH_2(\tilde{X}\,^2B_1)$ observed in the photolysis of a 5 mTorr HNCO/0.67 Torr H_2 mixture.: (a) (0,0,0) vibrational level for 9.33 Torr He buffer; (b) (0,1,0) for 9.33 Torr He buffer; (c) (0,0,0) for 1 Torr CF_4+8.33 Torr He buffer. Dashed curve is the calculated profile for total NH_2 using $k_1=4.0\times10^{-12}$ cm^3 $molecule^{-1}$ s^{-1}, which is obtained by the decay rate of $NH(a\,^1\Delta)$.

$NH(a\,^1\Delta)$ in this case. Evidently addition of CF_4 accelerated the relaxation of vibrationally excited NH_2 produced in reaction (1).

Such trends can be more clearly seen in Fig. 8, where the formation rate (defined as the inverse of time required to reach 1–1/e of the steady level) of $NH_2(\tilde{X})(0,0,0)$ is plotted against $[H_2]$. The formation rate without addition of CF_4 increased linearly (the dashed line), but the slope is much less than that expected from the decay of $NH(a\,^1\Delta)$. However, addition of 1 Torr CF_4 resulted in almost the same dependence of NH_2 formation rate on $[H_2]$ until the rate exceeded 8×10^4 s^{-1}, as denoted by the solid line. It should be noted that addition of CF_4 did not affect the $NH(a\,^1\Delta)$ profiles, and also electronic quenching process of $NH(a\,^1\Delta)$ was negligible since no LIF signal of $NH(X\,^3\Sigma^-)$ was observed.

Addition of 1 Torr SF_6 or variation of pressure of He in the range 5–50 Torr did not affect the rise rate of $NH_2(\tilde{X})(0,0,0)$ significantly. The kinetic measurement of NH_2 at higher pressure was not possible due to the very fast collisional quenching of $NH_2(\tilde{A})$.[44] This implies that both SF_6 and He are inefficient quenchers for the vibrationally excited NH_2. H_2 is a more effective quencher than SF_6 or He, but less effective than CF_4. From an analysis for the decay part of $NH_2(\tilde{X})(0,1,0)$ as a function of H_2 concentration, the relaxation rate constant of NH_2 by H_2 was obtained as $(4.8\pm1.5)\times10^{-13}$ cm^3 $molecule^{-1}$ s^{-1}. This result is consistent with the literature value (5.3×10^{-13}) for O_2 as the collision partner.[45] Relaxation by CF_4 is estimated as five times faster than that by H_2 assuming that the saturated rate of 8×10^4 s^{-1} shown in Fig. 8 represents the relaxation rate by 1 Torr CF_4.

This is the first direct demonstration that vibrationally excited NH_2 was formed in a reaction involving $NH(a\,^1\Delta)$. In an earlier observation Paur and Bair[2] found an incubation time of about 20 μs for $NH_2(\tilde{X})$ formation

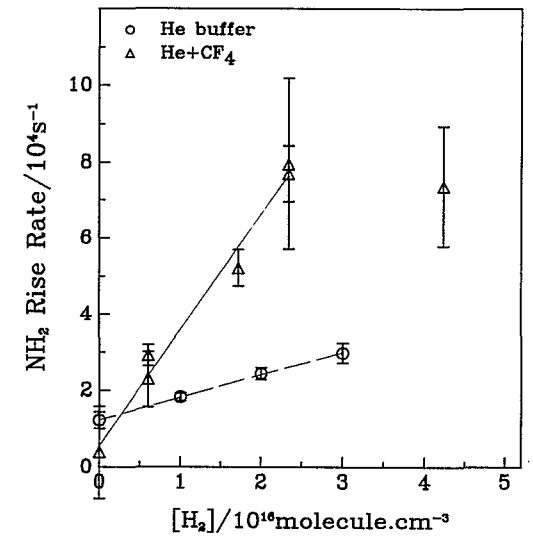

FIG. 8. $NH_2(\tilde{X}\,^2B_1)(0,0,0)$ rise rate as a function of H_2 concentration. Circles for He buffer; triangles for 1 Torr CF_4+He buffer (10 Torr total pressure). Solid and dashed curves are results of least squares fit.

in the $NH(a\ ^1\Delta)+HN_3$ reaction using resonant absorption in a discharge flash photolysis of HN_3 buffered by excess amount of Ar. They attributed this to generation of vibrationally excited NH_2 through the dependence of NH_2 formation rate on the total pressure up to 500 Torr. Afterwards Baronavski *et al.*[3] observed chemiluminescence from $NH_2(\tilde{A}\ ^2A_1)$ in 266 nm laser flash photolysis of HN_3, where onset of the emission was in agreement with the corresponding decay of $NH(a\ ^1\Delta)$, but they could not detect $NH_2(\tilde{X}\ ^2B_1)$ by means of a LIF technique. Consequently, they claimed that production of electronically excited NH_2 is the major process in reaction of $NH(a\ ^1\Delta)$ and HN_3.

IV. INFORMATION THEORETIC APPROACH

Product branching fraction in reaction (2) and vibrational excitation in NH_2 as a product of reaction (1) are discussed in the following in terms of the information theoretic procedure.[46]

A. Product branching fraction in $NH(a\ ^1\Delta)+D_2$

The products for the two channels of reaction (2) are the combinations of a nonlinear triatomic molecule and an atom, NHD+D (2a) and ND_2+H (2b). The potential energy surfaces are the same for reactions (2a) and (2b), except for their zero point energies due to the different mass combinations. Each pair of the products has three vibrational degrees of freedom and three rotational degrees of freedom.

The density of states at a given translational energy E_t is given by

$$\rho_t(E_t)=A_tE_t^{1/2},\quad A_t=\mu^{3/2}/2^{1/2}\pi^2h^3. \tag{4}$$

In the rigid-rotor (RR) approximation, summation over rotational states can be replaced by integrations as

$$\rho(E_v;E)=\iiint \rho_a\rho_b\rho_c\rho_t(E-E_v-E_R)dE_a\,dE_b\,dE_c$$
$$=\frac{8}{105}\frac{\mu^{3/2}}{2^{1/2}\pi^2h^6c^3}\frac{1}{ABC}(E-Ev)^{7/2}, \tag{5}$$

where ρ_i $(i=a,b,c)$ is the rotational density of states,

$$\rho_i=(2J_i+1)\frac{dJ_i}{dE_i}=1/(hcB_i). \tag{6}$$

When the harmonic oscillator (HO) approximation is added further, summation over vibrational states is replaced by

$$\rho_0(E)=\iiint dE_1\,dE_2\,dE_3\,\rho(Ev;E)/(\omega_1\omega_2\omega_3)$$
$$=\frac{64}{135135}\frac{\mu^{3/2}}{2^{1/2}\pi^2h^6c^3}\frac{1}{ABC}\frac{1}{\omega_1\omega_2\omega_3}E^{13/2}. \tag{7}$$

Consequently, the prior branching fraction is obtained as the ratio $2\rho_0(E';\mathrm{NHD+D})/\rho_0(E'';\mathrm{ND_2+H})$. Here E' and E'' in this ratio should be corrected for the zero point energy of NHD and ND_2, respectively.

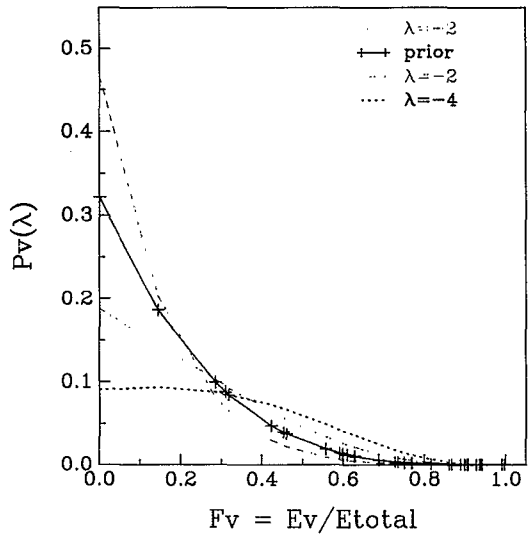

FIG. 9. Calculated vibrational distributions of $NH_2(\tilde{X}\ ^2B_1)$ using Eq. (8) in the text for prior ($\lambda=0$; solid curve) and biased (broken curves) distributions. Crosses in the solid curve indicate the positions of the vibrational levels.

Using molecular constants in the literature[40–43,47] and 29.7 kcal/mol for the total energy $E(NH_2+H)$ [heat of reaction plus entrance activation energy of 1.5 kcal/mol (Refs. 15, 48)], the prior branching fraction is calculated to be 0.97 (=0.49/0.51). The D/H ratio obtained experimentally in this work, 3.12 ± 0.60, is about three times more favorable toward the NHD+D channel.

B. Product vibrational distribution and vibrational relaxation of $NH_2(\tilde{X})$ in reaction (1)

Thirty-three levels of vibration are available assuming 29.7 kcal/mol of total energy in the product NH_2+H. The prior vibrational distribution $P_0(v)$ using the RR approximation is obtained by normalization of $\rho(Ev;E)$ of Eq. (5), and a biased (nonstatistical) distribution is expressed employing a surprisal parameter λ as

$$P(v;\lambda)=P_0(v)e^{-\lambda f_v}/\left\{\sum_v P_0(v)e^{-\lambda f_v}\right\}, \tag{8}$$

where $f_v=E_v/E_{\mathrm{total}}$. Examples of calculated biased distributions are shown in Fig. 9. Population in the vibrational ground state is 32% in the prior case.

Vibrational relaxation of NH_2 proceeding simultaneously with reaction (1) was simulated assuming the energy gap law for the vibrational energy transfer rate constants,

$$k(v\rightarrow v')=Ae^{-\alpha\Delta E_{vv'}/\mathrm{kT}}=k_{10}e^{-\alpha(\Delta E_{vv'}-\Delta E_{10})/\mathrm{kT}}, \tag{9}$$

$$k(v'\rightarrow v)=e^{-\Delta E_{vv'}/\mathrm{kT}}k(v\rightarrow v'),\quad (v>v'), \tag{10}$$

where k_{10} is the relaxation rate constant from (0,1,0) to (0,0,0) and $\Delta E_{vv'}=E_v-E_{v'}$. Here the three vibrational degrees of freedom were treated as a single mode and counted simply in order of their energy levels.

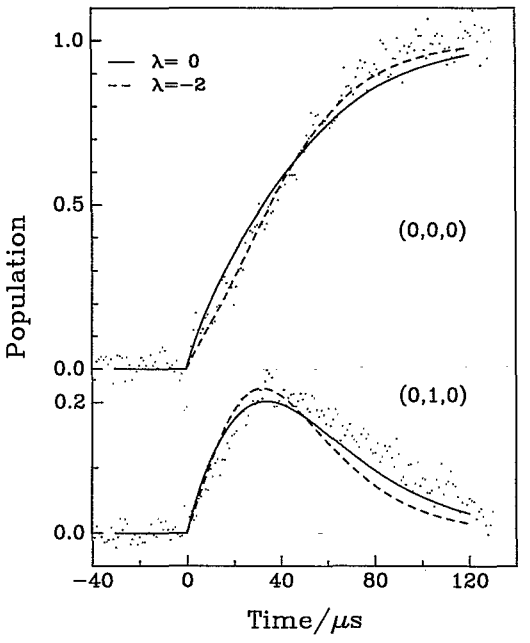

FIG. 10. A comparison of the calculated $NH_2(\tilde{X}\,^2B_1)$ profiles for the $NH(a\,^1\Delta)+H_2$ reaction in 10 Torr He with experiment at $[H_2]=2.0\times10^{16}$ molecule cm^{-3}. k_{10} (relaxation rate constant with H_2) was determined to be: 2.2×10^{-12} cm^3 $molecule^{-1}$ s^{-1} for $\lambda=0$, and 2.9×10^{-12} cm^3 $molecule^{-1}$ s^{-1} for $\lambda=-2$; α was assumed to be 0.5.

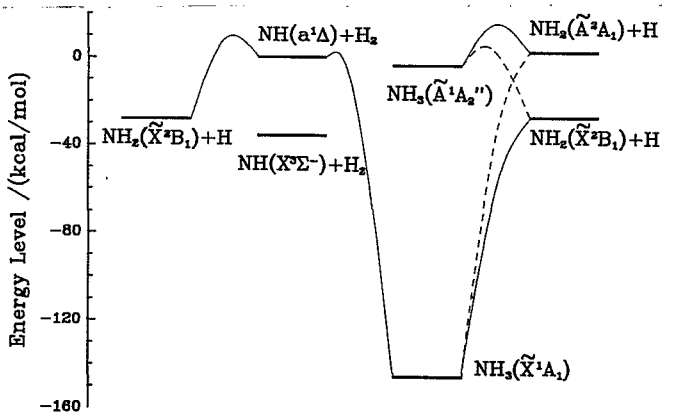

FIG. 11. The energy level diagram for the reactions of the NH–H_2 system. The adiabatic dissociation paths from NH_3 to NH_2+H at the right side are shown by the solid curves in nonplanar (C_s) geometry, and the dashed curves in planar (C_{2v}) geometry.

To get a good fit in the simulation of the profiles for $NH_2(0,0,0)$ and $(0,1,0)$, the parameter k_{10} was found to have a close correlation to α; on the other hand, λ was nearly an independent parameter. In the present analysis, k_{10} was treated as a primary parameter and α as a secondary one. As shown in Fig. 10, the simulation curve with $\lambda\sim0$ to -2 could reproduce the observed profiles well, especially in the trapezoidal shape of the (0,0,0) profile. As shown in Fig. 9, the estimated range of λ yields the nascent population in the (0,0,0) state as 20%–30%. It should also be noted that the ratio of the initial rising slope of the (0,0,0) profile (within 20 μs after the incidence of photolysis), to the overall NH_2 production rate is approximately the same as the nascent fraction in the (0,0,0) state, regardless of what nascent distribution was assumed or the occurrence of relaxation from states higher than (0,1,0). From this point of view, it is also deduced that 20%–30% of the total NH_2 is produced directly in the (0,0,0) state in reaction (1).

V. DISCUSSION

The results of this study on the isotope effect for the overall rate constant, k_2/k_1, and the branching fraction for producing H and D atoms in reaction (2) indicate the presence of insertion as a main reaction mechanism in the $NH(a\,^1\Delta)+H_2$ or D_2 reactions. In addition, the observed product species, i.e., H(D) atom and $\tilde{X}\,^2B_1$ state of NH_2 (NHD, ND_2) are identified as the main products.

The potential energy levels relevant to reaction (1) are shown in Fig. 11. Besides the insertion path through $NH_3(\tilde{X}\,^1A_1)$ out to $NH_2(\tilde{X}\,^2B_1)$ as the minimum energy path, $NH_3(\tilde{A}\,^1A_2'')$ and $NH_2(\tilde{A}\,^2A_1)$ are thermochemically allowed as an intermediate and a final product, respectively.

Ab initio CI calculations were performed by Fueno *et al.* for the $NH(a\,^1\Delta)+H_2$ reaction path.[49–51] According to their most recent calculation where the MRD-CI/6–31G^{**} scheme was employed,[51] the barrier height is 2.9 and 5.8 kcal/mol for insertion and direct abstraction, respectively. Thus the abstraction seems still competitive though the insertion is considered to be dominant. On the insertion path, $NH(a\,^1\Delta)+H_2$ correlates to the formation of $NH_3(\tilde{X}\,^1A_1)$ if C_s symmetry is maintained. Although correlation to the first excited state of $NH_3(\tilde{A}\,^1A_2'')$ is uncertain, the barrier height between $NH(a\,^1\Delta)+H_2$ and $NH_3(\tilde{A}\,^1A_2'')$ must lie higher than that between $NH_3(\tilde{A}\,^1A_2'')$ and NH_2+H because production of $NH(a\,^1\Delta)$ in NH_3 photolysis was reported to be an extremely minor channel.[52,53]

For the dissociation of NH_3, an *ab initio* calculation was conducted by McCarthy *et al.*[48] As shown in Fig. 11, ground state $NH_3(\tilde{X}\,^1A_1)$ correlates with ground state $NH_2(\tilde{X}\,^2B_1)+H$ in C_s symmetry, and with excited state $NH_2(\tilde{A}\,^2A_1)$ in planar C_{2v} symmetry. On the other hand, reverse relationships hold for excited $NH_3(\tilde{A}\,^1A_2'')$ which has a planar (D_{3h}) equilibrium geometry. There exists a conical crossing of the $\tilde{A}$ and $\tilde{X}$ surfaces at 0° in the H–NH_2 out-of-plane angle. In NH_3 photolysis,[54–57] the downward path to the ground state $NH_2(\tilde{X}\,^2B_1)$ through surface hopping around the conical crossing is known to be a major channel. In the case of this study, the upward process from $NH_3(\tilde{X}\,^1A_1)$ to $NH_2(\tilde{A}\,^2A_1)$ seems far less probable than to $NH_2(\tilde{X}\,^2B_1)$, even if the $NH_3(\tilde{X})^*$ has enough internal energy.

It has been shown in this study, that the D/H branching ratio in reaction (2) is larger than the ratio of the statistical weights for the two channels. This may be due to a contribution of the abstraction channel forming D atoms preferentially, or due to a nonstatistical dissociation of

NHD_2 after the insertion. If the latter is true, the exothermicity is accumulated mostly in the newly created N–D bonds at the incidence of the insertion, then the molecule decomposes before the energy is partitioned in the old N–H bond. This is in contrast with the near-threshold photolysis of NHD_2 at around 210 nm,[57,58] where dissociation to give an H atom was reported to be several times faster than that forming a D atom due to the tunneling through the exit barrier to dissociation of the $\tilde{A}$ state of NHD_2. In order to evaluate the contribution of the abstraction process, it will be helpful to measure the temperature dependence of the H/D ratio for reaction (2).

Analysis of the partitioning of excess energy in the exit channel has shown that the product NH_2 vibration is nearly statistically excited. There remains some uncertainty in this analysis regarding the possibility of a selective excitation among vibrational modes. If the bending mode were selectively excited, for example, a larger negative surprisal parameter ($-\lambda$) would be required to fit the experimental time profiles. The present study indicated almost the same value on the vibrational surprisal for $NH(a\,^1\Delta)+H_2$ as found for reactions of $O(^1D)$. That is, λ is found to be about 0 for the $O(^1D)+H_2$ reaction whereas it is -7.3 for $O(^1D)+CH_4$ reaction.[36]

ACKNOWLEDGMENTS

We acknowledge Professor T. Fueno (Osaka University) and Professor S. Koda (University of Tokyo) for their helpful discussions.

[1] R. J. Paur and E. J. Bair, J. Photochem. **1**, 255 (1973).
[2] R. J. Paur and J. Bair, Int. J. Chem. Kinet. **8**, 134 (1976).
[3] (a) J. R. McDonald, R. G. Miller, and A. P. Baronavski, Chem. Phys. **30**, 119 (1978), (b) *ibid.* **30**, 133 (1978).
[4] W. S. Drozdoski, A. P. Baronavski, and J. R. McDonald, Chem. Phys. Lett. **64**, 421 (1979).
[5] H. H. Nelson, J. R. McDonald, and M. H. Alexander, J. Phys. Chem. **94**, 3291 (1990).
[6] O. Kajimoto and T. Fueno, Chem. Phys. Lett. **80**, 484 (1981).
[7] O. Kondo, J. Miyata, O. Kajimoto, and T. Fueno, Chem. Phys. Lett. **88**, 424 (1982).
[8] F. Freitag, F. Rohrer, and F. Stuhl, J. Phys. Chem. **93**, 3170 (1989).
[9] W. Hack and A. Wilms, Z. Phys. Chem. **161**, 107 (1989).
[10] W. Hack and A. Wilms, J. Phys. Chem. **93**, 3540 (1989).
[11] W. Hack and K. Rathman, J. Phys. Chem. **94**, 3636 (1990).
[12] W. Hack and K. Rathman, J. Phys. Chem. **94**, 4155 (1990).
[13] W. Hack and K. Rathman, Ber. Bunsenges. Phys. Chem. **94**, 1304 (1990).
[14] K. Yamasaki, S. Okada, M. Koshi, and H. Matsui, J. Chem. Phys. **95**, 5087 (1991).
[15] J. W. Cox, H. H. Nelson, and J. R. McDonald, Chem. Phys. **96**, 175 (1985).
[16] R. D. Bower, M. T. Jacoby, and J. A. Blauer, J. Chem. Phys. **86**, 1954 (1987).
[17] F. Freitag, F. Rohrer, and F. Stuhl, J. Phys. Chem. **93**, 3170 (1989).
[18] J. A. Davidson, H. I. Schiff, G. E. Streit, J. R. McAfee, A. L. Schmeltekopf, and C. J. Howard, J. Chem. Phys. **67**, 5021 (1977).
[19] W. Braun, A. M. Bass, and M. Pilling, J. Chem. Phys. **52**, 5131 (1970).
[20] M. N. R. Ashfold, M. A. Fullstone, G. Hancock, and G. W. Ketley, Chem. Phys. **55**, 245 (1981).
[21] A. O. Langford, H. Petek, and C. B. Moore, J. Chem. Phys. **78**, 6650 (1983).
[22] G. K. Smith, J. E. Butler, and M. C. Lin, Chem. Phys. Lett. **65**, 115 (1979).
[23] G. K. Smith and J. E. Butler, J. Chem. Phys. **73**, 2243 (1980).
[24] J. E. Butler, G. M. Jursich, I. A. Watson, and J. R. Wiesenfeld, J. Chem. Phys. **84**, 5365 (1986).
[25] C. B. Cleveland, G. M. Jursich, M. Trolier, and J. R. Wiesenfeld, J. Chem. Phys. **86**, 3253 (1987).
[26] A. Lebehot, S. Drawin, F. Aguillon, and R. Campargue, J. Chem. Phys. **92**, 7340 (1990).
[27] K. Tsukiyama, B. Katz, and R. Bersohn, J. Chem. Phys. **83**, 2989 (1985).
[28] P. A. Whitlock, J. T. Muckerman, and R. E. Fisher, J. Chem. Phys. **76**, 4468 (1982).
[29] R. E. Howard, A. E. Mclean, and W. A. Lester, Jr., J. Chem. Phys. **71**, 2412 (1979).
[30] R. Schinke and W. A. Lester, Jr., J. Chem. Phys. **72**, 3754 (1980).
[31] J. N. Murrell, S. Carter, I. M. Mills, and M. F. Guest, Mol. Phys. **42**, 605 (1981).
[32] J. N. Murrell and S. Carter, J. Phys. Chem. **88**, 4887 (1984).
[33] W. Ransome and J. S. Wright, J. Chem. Phys. **77**, 6346 (1982).
[34] M. S. Fitzcharles and G. C. Schatz, J. Phys. Chem. **90**, 3634 (1986).
[35] L. J. Dunne, Chem. Phys. Lett. **158**, 535 (1989).
[36] A. C. Luntz, J. Chem. Phys. **73**, 1143 (1980).
[37] M. Koshi, F. Tamura, and H. Matsui, Chem. Phys. Lett. **173**, 235 (1990).
[38] T. A. Spiglanin, R. A. Perry, and D. W. Chandler, J. Phys. Chem. **90**, 6184 (1986).
[39] K.-H. Gericke, M. Lock, and F. J. Comes, Chem. Phys. Lett. **186**, 427 (1991).
[40] K. Dressler and D. A. Ramsay, Philos. Trans. R. Soc. London Ser. A **251**, 553 (1959).
[41] S. C. Ross, F. W. Birss, M. Vervloet, and D. A. Ramsay, J. Mol. Spectrosc. **129**, 436 (1988).
[42] D. A. Ramsay and F. D. Wayne, Can. J. Phys. **57**, 761 (1979).
[43] M. Vervloet, M. F. Merienne-Lafore, and D. A. Ramsay, Chem. Phys. Lett. **57**, 5 (1978).
[44] J. B. Halpern, G. Hancock, M. Lenzi, and K. H. Welge, J. Chem. Phys. **63**, 4808 (1975).
[45] K.-H. Gericke, L. M. Torres, and W. A. Guillory, J. Chem. Phys. **80**, 6134 (1984).
[46] (a) I. Procaccia and R. D. Levine, J. Chem. Phys. **63**, 4261 (1975); (b) R. D. Levine and J. L. Kinsey, in *Atom–Molecule Collision Theory, A Guide for the Experimentalist*, edited by R. B. Bernstein (Plenum, New York, 1979).
[47] CH. Jungen, K.-E. J. Hallin, and A. J. Merer, Mol. Phys., **40**, 25 (1980).
[48] M. I. McCarthy, P. Rosmus, H.-J. Werner, P. Botschwina, and V. Vaida, J. Chem. Phys. **86**, 6693 (1987).
[49] T. Fueno, V. Bonacic-Koutecky, and J. Koutecky, J. Am. Chem. Soc. **105**, 5547 (1983).
[50] T. Fueno, O. Kajimoto, and V. Bonacic-Koutecky, J. Am. Chem. Soc. **106**, 4061 (1984).
[51] T. Fueno (private communication).
[52] H. Okabe and M. Lenzi, J. Chem. Phys. **47**, 5241 (1967).
[53] V. M. Donnelly, A. P. Baronavski, and J. R. McDonald, Chem. Phys. **43**, 271 (1979).
[54] E. L. Woodbridge, M. N. R. Ashfold, and S. R. Leone, J. Chem. Phys., **94**, 4195 (1991).
[55] J. Biesner, L. Schnieder, J. Schmeer, G. Ahlers, X. Xie, K. H. Welge, M. N. R. Ashfold, and R. N. Dixon, J. Chem. Phys. **88**, 3607 (1988).
[56] J. Biesner, L. Schnieder, G. Ahlers, X. Xie, K. H. Welge, M. N. R. Ashfold, and R. N. Dixon, J. Chem. Phys. **91**, 2901 (1989).
[57] K. Fuke, H. Yamada, Y. Yoshida, and K. Kaya, J. Chem. Phys. **88**, 5238 (1988).
[58] A. Nakajima, K. Fuke, K. Tsukamoto, Y. Yoshida, and K. Kaya, J. Phys. Chem. **95**, 571 (1991).